Compton Camera Imaging

Shiro Ikeda*, Hirokazu Odaka†, Makoto Uemura‡, Tadayuki Takahashi† Shin Watanabe† and Shin'ichiro Takeda†

* The Institute of Statistical Mathematics & The Graduate Univ. for Advanced Studies
Tokyo, 106-8569, Japan
Email: shiro@ism.ac.jp

† Institute of Space and Astronautical Science
Japan Aerospace Exploration Agency
Kanagawa, 252-5210 Japan

‡ Astrophysical Science Center
Hiroshima University
Hiroshima, 739-8511 Japan

***Abstract*—The goal of the Compton camera imaging is to visualize the gamma-ray intensity map. Here, we focus on the case where the gamma-ray sources are sufficiently far from the camera and propose a new reconstruction method for the Compton camera imaging. The method is called the bin-mode estimation (BME). The assumption is valid for astronomy applications. The method can be implemented easily, and numerical simulations show the proposed method provides sharp reconstructions.**

keywords: Compton camera, image reconstruction, maximum likelihood estimation

I. Introduction

For visualization of the gamma-ray sources, the Compton camera imaging is an important approach. The applications of gamma-ray source visualization are widely spread, such as nuclear medicine, visualization of radioactive substances on the ground, and gamma-ray astronomy [1]–[5]. High-resolution Compton cameras with silicon (Si) and cadmium telluride (CdTe) semiconductor detectors have been developed [6]–[8], and will be installed in the next-generation X-ray observatory ASTRO-H [9], [10], which is scheduled for launch in 2015.

The imaging of Compton camera is not straightforward because 1) only a small portion of photons are absorbed after the Compton scattering and 2) not their direction of arrival but only the scattering angle is known from measurement. Some computational method must be applied in order to reconstruct the image.

In this paper, we introduce the bin-mode estimation (BME) method for the reconstruction. The bin-mode itself has already been introduced [1], [11]–[13], but has been only used in a limited case, because the number of bins become large for implementation [14], [15]. Here we focus on the astronomy application, where the distances from the gamma-ray sources are large, and show that the number of bins can be reduced to a tractable size. Under the assumption, the BME is a promising method for reconstruction. We propose the maximum likelihood estimation (MLE) with the expectation maximization (EM) algorithm. The proposed BME method is tested with simulation. The results show sharp images, which proves the method is promising.

This work was supported by JSPS Grant-in-Aid for Scientific Research on Innovative Areas, Number 25120008.

II. Compton camera imaging

A. Compton camera system

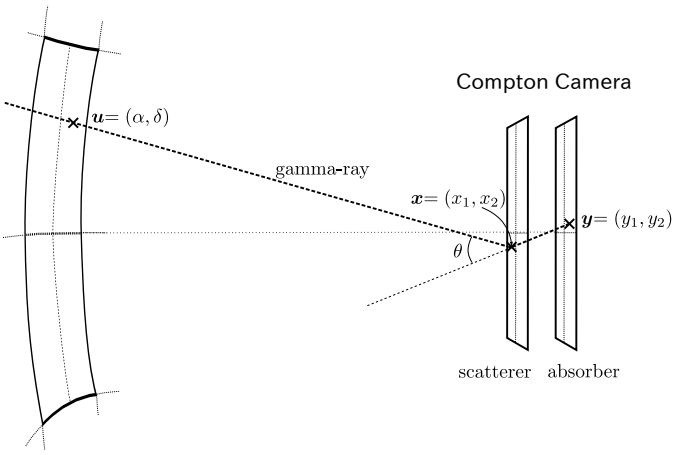

Fig. 1. Compton camera.

In figure 1, we show the Compton camera system with a single pair of scatterer and absorber. When a number of photons arrive, most of them are not absorbed by the absorber and a small portion of them are detected after Compton scattering. We assume the distance from the Compton camera system to each gamma-ray source is sufficiently large, and only consider the direction of arrival. This assumption is valid for the astronomy application.

Suppose a photon from $\boldsymbol{u} = (\alpha, \delta)$ (in equatorial coordinate) is detected. It is first scattered by the scatterer at $\boldsymbol{x} = (x_1, x_2)$ and then is absorbed by the absorber at $\boldsymbol{y} = (y_1, y_2)$. Let E_1 and E_2 be the energies of the recoil electron and of the scattered photon, respectively. The scattering angle θ has the following relation with E_1 and E_2

$$\cos\theta = 1 - m_e c^2 \left(\frac{1}{E_2} - \frac{1}{E_1 + E_2} \right),$$

where m_e and c are the mass of an electron and the speed of light, respectively.

The goal of Compton camera imaging is to reconstruct the gamma-ray intensity map on the celestial sphere from

collected information. The difficulty arises because not the direction of arrival but only the angle of scattering is provided by each measurement.

Under the assumption that the distances from the camera to each source is large, not both of $\boldsymbol{x}$ and $\boldsymbol{y}$, but only the relative position $\boldsymbol{w} = \boldsymbol{x} - \boldsymbol{y}$ is important because each direction of arrival corresponds to a single point on the celestial sphere. The information of each detected photon is summarized into $\boldsymbol{v} = (\boldsymbol{w}, \cos\theta)$.

B. Compton camera measurement process

In the following, we assume $\boldsymbol{u} = (\alpha, \delta)$ and $\boldsymbol{v}$ are quantified into bins. Thus, $\boldsymbol{u}$ and $\boldsymbol{v}$ are bin indices.

When a gamma-ray photon from $\boldsymbol{u}$ is detected, it falls into a bin $\boldsymbol{v}$ with some probability. We introduce the probabilistic formulation. We first introduce a formulation of the measurement process [14], [15]. Let $\lambda(\boldsymbol{u})$ be the intensity of the gamma rays at pixel $\boldsymbol{u}$ of the celestial sphere and $Y(\boldsymbol{v})$ be the number of photons detected at bin $\boldsymbol{v}$ in a time interval. The distribution of $Y(\boldsymbol{v})$ follows a Poisson distribution, that is,

$$Y(\boldsymbol{v}) \sim \mathrm{Poisson}\left(\sum_{\boldsymbol{u}} t(\boldsymbol{v}, \boldsymbol{u})\ \lambda(\boldsymbol{u}) \right), \tag{1}$$

where a matrix $t(\boldsymbol{v}, \boldsymbol{u})$ gives the probability that a photon from pixel $\boldsymbol{u}$ is absorbed at bin $\boldsymbol{v}$.

We next modify the formulation in eq. (1). Let us re-parameterize $t(\boldsymbol{v}, \boldsymbol{u})$ and $\lambda(\boldsymbol{u})$ as follows,

$$p(\boldsymbol{v} \,|\, \boldsymbol{u}) = \frac{t(\boldsymbol{v}, \boldsymbol{u})}{s(\boldsymbol{u})} \quad \text{where} \quad s(\boldsymbol{u}) = \sum_{\boldsymbol{v}} t(\boldsymbol{v}, \boldsymbol{u}),$$
$$\rho(\boldsymbol{u}) = \frac{\lambda(\boldsymbol{u}) s(\boldsymbol{u})}{\lambda} \quad \text{where} \quad \lambda = \sum_{\boldsymbol{u}} \lambda(\boldsymbol{u}) s(\boldsymbol{u}),$$

where $s(\boldsymbol{u})$ is the probability that a photon from pixel $\boldsymbol{u}$ is absorbed by the camera. We further define $q(\boldsymbol{v})$ as follows

$$q(\boldsymbol{v}) = \sum_{\boldsymbol{u}} p(\boldsymbol{v} \,|\, \boldsymbol{u})\, \rho(\boldsymbol{u}).$$

From the definition, all of $\rho(\boldsymbol{u})$, $p(\boldsymbol{v} \,|\, \boldsymbol{u})$, and $q(\boldsymbol{v})$ are non-negative and $\sum_{\boldsymbol{u}} \rho(\boldsymbol{u}) = 1$, $\sum_{\boldsymbol{v}} p(\boldsymbol{v} \,|\, \boldsymbol{u}) = 1$, and $\sum_{\boldsymbol{v}} q(\boldsymbol{v}) = 1$. All of $\rho(\boldsymbol{u})$, $p(\boldsymbol{v} \,|\, \boldsymbol{u})$, and $q(\boldsymbol{v})$ are multinomial distributions conditional to the event that a photon is absorbed by the camera. More precisely, under the condition, $\rho(\boldsymbol{u})$ is the probability that a photon arrives from $\boldsymbol{u}$, $p(\boldsymbol{v} \,|\, \boldsymbol{u})$ is the probability that a photon from $\boldsymbol{u}$ is absorbed at $\boldsymbol{v}$, and $q(\boldsymbol{v})$ is the probability that a photon is absorbed at $\boldsymbol{v}$.

Although the distribution $\rho(\boldsymbol{u})$ is different from $\lambda(\boldsymbol{u})$, the intensity map is easily reconstructed as follows assuming $s(\boldsymbol{u})$ is known,

$$\lambda(\boldsymbol{u}) \propto \frac{\rho(\boldsymbol{u})}{s(\boldsymbol{u})}.$$

Here, we neglected the factor λ because it is not important for the image reconstruction.

The photons which are not absorbed by the absorber are ignored in the modified formulation. The number of absorbed photons in a time interval is a stochastic variable which follows $\mathrm{Poisson}(\lambda)$.

III. BME method

Now, we discuss the estimation method of $\rho(\boldsymbol{u})$ from observed photon counts.

Consider the case where N photons are detected and t-th photon is absorbed at $\boldsymbol{v}_t$, $(t = 1, \cdots, N)$. Assuming each photon arrives independently, the log likelihood function is

$$L(\rho) = \sum_{t=1}^{N} \log\ q(\boldsymbol{v}_t) = \sum_{t=1}^{N} \log \sum_{\boldsymbol{u}} p(\boldsymbol{v}_t \,|\, \boldsymbol{u})\ \rho(\boldsymbol{u}).$$

Le us assume $p(\boldsymbol{v} \,|\, \boldsymbol{u})$ is known and the EM algorithm [16] can be used to estimate $\rho(\boldsymbol{u})$. The distribution $\rho(\boldsymbol{u})$ is updated with the EM iteration as follows,

$$\begin{aligned} q^{(l)}(\boldsymbol{v}) &= \sum_{\boldsymbol{u}} p(\boldsymbol{v} \,|\, \boldsymbol{u})\ \rho^{(l)}(\boldsymbol{u}), \\ \rho^{(l+1)}(\boldsymbol{u}) &= \frac{1}{N} \sum_{t=1}^{N} \frac{p(\boldsymbol{v}_t \,|\, \boldsymbol{u})}{q^{(l)}(\boldsymbol{v}_t)}\ \rho^{(l)}(\boldsymbol{u}), \end{aligned} \tag{2}$$

where l is the number of the iteration starting from 0 and increasing by 1 at each iteration. The log-likelihood is non-decreasing during the updates, that is, $L(\rho^{(l+1)}) \geq L(\rho^{(l)})$. The maximum likelihood estimate (MLE) is obtained when the EM algorithm converges. Let us denote it as $\hat{\rho}_{\mathrm{MLE}}(\boldsymbol{u})$. The reconstructed image is proportional to $\hat{\rho}_{\mathrm{MLE}}(\boldsymbol{u})/s(\boldsymbol{u})$. We note that a naive estimate of λ is N.

Our formulation is based on bin-mode, that is, each of $\boldsymbol{v}$ and $\boldsymbol{u}$ is quantified into bins. The key for the implementation of eq. (2) is the conditional distribution matrix $p(\boldsymbol{v} \,|\, \boldsymbol{u})$. We have assumed this distribution is known, but it has been pointed out that the size of $p(\boldsymbol{v} \,|\, \boldsymbol{u})$ is so large for bin-mode that it cannot be prepared in advance, and cannot be used for estimation [14], [15].

If $\boldsymbol{x}$, $\boldsymbol{y}$, E_1, and E_2 are quantified separately, the number of bins becomes large and bin-mode is intractable. We have made an assumption that the distances from the sources of gamma rays are sufficiently large and the information of the detection is summarized into $(\boldsymbol{w}, \cos\theta)$. Under this assumption, we quantify $(\boldsymbol{w}, \cos\theta)$ instead of $(\boldsymbol{x}, \boldsymbol{y}, E_1, E_2)$ so that the number of bins decreases. The matrix $p(\boldsymbol{v} \,|\, \boldsymbol{u})$ becomes tractable under this treatment.

Now, the problem is how to prepare $p(\boldsymbol{v} \,|\, \boldsymbol{u})$ and $s(\boldsymbol{u})$. In this work, we utilized a numerical method. A Compton camera system is simulated and a lot of photons are randomly drawn by numerical simulation. The results are accumulated to compute $p(\boldsymbol{v} \,|\, \boldsymbol{u})$ and $s(\boldsymbol{u})$. Modern computers are so fast that sufficiently large number of samples can be collected easily by running in parallel. This method is general and implementation is easy.

IV. Numerical Results

A. Simulated Compton camera

A simple Compton camera, which consists of a Si pixel detector as the scatterer and a CdTe pixel detector as the absorber, is employed for numerical experiments. Each detector

is pixellated into 32×32 channels, and has an energy resolution of 2 keV (full width at half maximum). The sizes of scatterer and absorber are identical: 64 mm square and 2.0 mm thick. They are located 20 mm apart. The physical parameters of them are summarized in table I.

TABLE I
PHYSICAL PARAMETERS OF THE SIMULATED SEMI-CONDUCTOR.

		density [g cm^{-3}]	energy resolution FWHM[keV]
scatterer	Si	2.33	2.0
absorber	CdTe	5.86	2.0

A physical model of the Compton camera is constructed by particle tracking simulations, in other words, by Monte Carlo simulations. We used our Compton camera response generator [17], which are implemented with the Geant4 toolkit (Version 9.6.p01) [18] on a desktop computer (Mac Pro 6-core Intel Xeon 3.33 GHz). The simulations accurately treat the Doppler broadening effect of Compton scattering [19], which is caused by non-zero momentum of a target electron and degrades angular resolutions of the Compton camera.

TABLE II
DESIGN OF BINS OF $\boldsymbol{u}$ AND $\boldsymbol{v}$.

	$\boldsymbol{u}$		$\boldsymbol{v}$		
	α	δ	$\frac{w_1}{\sqrt{\lvert w_1\rvert}}$	$\frac{w_2}{\sqrt{\lvert w_2\rvert}}$	$\cos\theta$
	[degree]		[mm$^{1/2}$]		
min	-30	-30	-8.2	-8.2	$-.24$
max	30	30	8.2	8.2	.96
# of bins	21	21	17	17	24

The designs of bins are summarized in table II. Angles α, δ, and $\cos\theta$ are quantified into equally spaced bins. For relative positions w_1 and w_2, equal space is not preferable because the number of photons absorbed at the center is larger than at the boundaries. In order to prevent such unbalanced situation, the square roots of w_1 and w_2 are quantified into equally spaced bins. The total numbers of bins of $\boldsymbol{u}$ and $\boldsymbol{v}$ are $21\times21=441$ and $17\times17\times24=6,936$, respectively.

A large number, 6.4×10^{10} of photons are randomly generated and recorded in order to compute $p(\boldsymbol{v}\,|\,\boldsymbol{u})$ and $s(\boldsymbol{u})$. The energy of gamma-ray photon is set to 661.7 keV (^{137}Cs). The number of detected photons is 9,774,163, that is, around .0153 % of the photons are finally absorbed by the absorber. The distributions $p(\boldsymbol{v}\,|\,\boldsymbol{u})$ and $s(\boldsymbol{u})$ are computed with these photon counts. One note is that the estimated $p(\boldsymbol{v}\,|\,\boldsymbol{u})$ has some 0's, which makes the EM algorithm unstable, and we replace 0's with a small constant, 1.0×10^{-10}. We have only considered ^{137}Cs in the current simulation, but this can be easily extended to other gamma-ray sources. It is also possible to apply the method even if multiple gamma-ray sources are mixed.

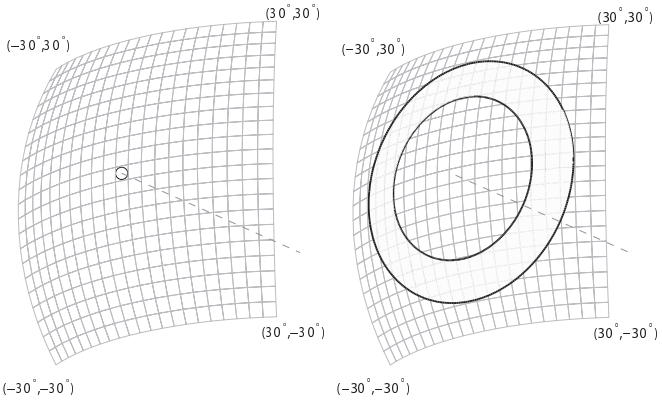

(a) Source A: single point source. (b) Source B: distributed source on a ring.

Fig. 2. Gamma-ray sources used for numerical simulations: (a) source A: the circle indicates the position of a point source at $(0°, 0°)$, and (b) source B: distributed source on a ring, whose inside and outside are $16°$ and $24°$ apart from the center, respectively. The dash lines in the figures indicate the direction of the Compton camera.

B. Image reconstruction

We prepared 2 types of gamma-ray sources for the numerical simulations of image reconstruction. They are shown in fig. 2. Source A is a single point source (fig. 2a), and source B is a distributed source on a ring-shaped region (fig. 2b).

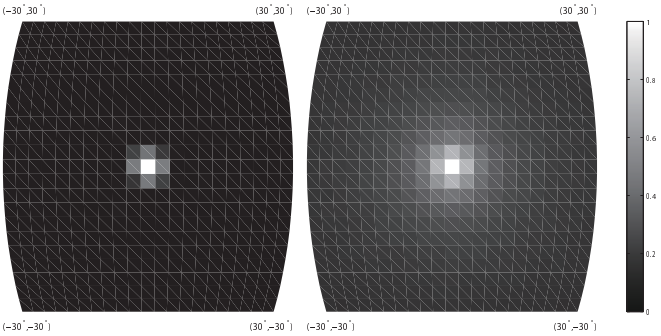

(a) MLE reconstruction. (b) Back projection reconstruction.

Fig. 3. Reconstructed images for source A in fig. 2a. 45,866 photons are absorbed. (a) the MLE reconstruction (all 441 pixels are positive), (b) image reconstruction with the back projection. Each image is normalized to have 1 as its maximum.

From each of the source models, numbers of photons are randomly generated, and images are reconstructed. We used the BM-MLE. We also show the results of back-projection for comparison.

Figure 3 shows the reconstructed images for source A. Each figure has its maximum at the center where a single point gamma-ray source is located. The BME gives sharp images while the back-projection reconstruction results in a blurred image.

The results for source B are shown in fig. 4. The difference between the BME and the back-projection becomes clear, that the inside of the ring s positive for the back projection, but BME is sharp and the edge of ring-shaped is well-preserved.

All of BME are implemented on a desktop computer (Intel Core i7-3770S, 3.10 GHz) with Matlab 2013a (Ubuntu Linux 13.04, x86-64). As the source becomes complicated, time for convergence of the EM algorithm becomes longer. For source A, the MLE is computed within 1 min, and that for source B, which is the complicated, is computed within 6 min.

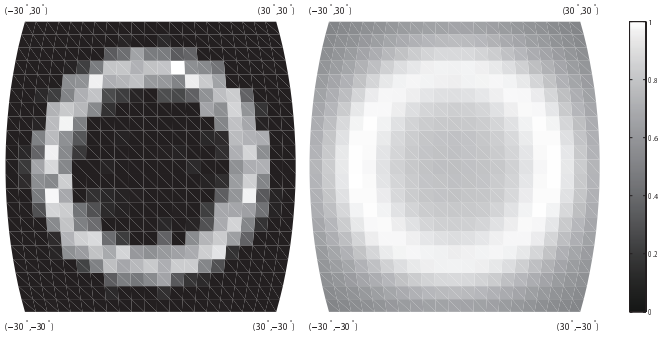

(a) MLE reconstruction. (b) Back projection reconstruction.

Fig. 4. Reconstructed images for source B in fig. 2b. 1,830,643 photons are absorbed. (a) the MLE reconstruction (441 pixels are positive), (b) image reconstruction with the back projection.

V. Conclusion

We have proposed a BME method for the Compton camera imaging. The method can be implemented easily, and the reconstructed images are sharp. The method is a promising candidate for astronomy applications.

It has been pointed out that the number of bins can become so large that the BME is not tractable. We have made an assumption that the distances from the gamma-ray sources are large. Under the assumption, the direction of the arrival is important, but the position where the photon hit the Compton camera is not important. This fact makes it possible to reduce the number of bins drastically, and the BME becomes possible.

Our goal is to apply the method to real systems. For real applications, we have to reduce the computational cost. The MLE is estimated with the EM algorithm, but it is known that the EM algorithm is slow. A lot of ideas for acceleration have been proposed for the EM algorithm [20], [21] and some of them would be applied in order to have faster convergence. Experiments with real data will be done in a near future.

References

[1] V. Schönfelder, *et al*., "COMPTEL overview: Achievements and expectations," *Astron. Astrophys. Suppl. Ser.*, vol. 120, pp. 13–21, 1996.

[2] J. LeBlanc, *et al*., "C-SPRINT: a prototype Compton camera system for low energy gamma ray imaging," *IEEE trans. Nucl. Sci.*, vol. 45, no. 3, pp. 943–949, 1998.

[3] T. Takahashi, *et al*., "High resolution CdTe detectors for the next-generation multi-Compton gamma-ray telescope," *Proc. SPIE*, vol. 4851, p. 1228, March 2003.

[4] G. Kanbach, *et al*., "The MEGA project," *New Astronomy Reviews*, vol. 48, no. 1, pp. 275–280, February 2004.

[5] S. E. Boggs, "The Advanced Compton Telescope mission," *New Astronomy Reviews*, vol. 50, no. 7-8, pp. 604–607, 2006.

[6] S. Watanabe, *et al*., "A Si/CdTe semiconductor Compton camera," *IEEE trans. Nucl. Sci.*, vol. 52, no. 5, pp. 2045–2051, 2005.

[7] S. Takeda, *et al*., "Experimental results of the gamma-ray imaging capability with a Si/CdTe semiconductor Compton camera," *IEEE trans. Nucl. Sci.*, vol. 56, no. 3, pp. 783–790, 2009.

[8] H. Odaka, *et al*., "High-resolution Compton cameras based on Si/CdTe double-sided strip detectors," *Nucl. Instr. and Meth. A*, vol. 695, pp. 179–183, 2012.

[9] T. Takahashi, *et al*., "The ASTRO-H mission," *Proc. SPIE*, vol. 7732, p. 77320Z, 2010.

[10] H. Tajima, *et al*., "Soft gamma-ray detector for the ASTRO-H mission," *Proc. SPIE*, vol. 7732, p. 773216, 2010.

[11] H. Bloemen, *et al*., "COMPTEL imaging of the Galactic disk and the separation of diffuse emission and point sources," *Astrophys. J. Suppl. Ser.*, vol. 92, no. 2, pp. 419–423, 1994.

[12] J. Knödlseder, *et al*., "Image reconstruction of COMPTEL 1.8 MeV^{26} Al line data," *Astron. Astrophys.*, vol. 345, pp. 813–825, 1999.

[13] M. Bandstra, *et al*., "Detection and imaging of the Crab Nebula with the nuclear Compton telescope," *The Astrophysical Journal*, vol. 738, no. 8, 2011, doi:10.1088/0004-637X/738/1/8.

[14] S. J. Wilderman, N. H. Clinthorne, J. A. Fessler, and W. L. Rogers, "List-mode maximum likelihood reconstruction of Compton scatter camera images in nuclear medicine," in *Proc. IEEE Nucl. Sci. Symp.*, 1998, pp. 1716–1720.

[15] ——, "Improved modeling of system response in listmode EM reconstruction of Compton scatter camera images," *IEEE trans. Nucl. Sci.*, vol. 48, no. 1, pp. 111–116, February 2001.

[16] A. P. Dempster, N. M. Laird, and D. B. Rubin, "Maximum likelihood from incomplete data via the EM algorithm," *J. R. Statistical Society, Series B*, vol. 39, pp. 1–38, 1977.

[17] H. Odaka and *et al*., "Development of an integrated response generator for Si/CdTe semiconductor Compton cameras," *Nucl. Instr. and Meth. A*, vol. 624, no. 2, pp. 303–309, December 2010.

[18] J. Allison and *et al*., "Geant4 developments and applications," *IEEE trans. Nucl. Sci.*, vol. 53, no. 1, pp. 270–278, February 2006.

[19] A. Zoglauer and G. Kanbach, "Doppler broadening as a lower limit to the angular resolution of next-generation Compton telescopes," *Proc. SPIE*, p. 1302, 2003.

[20] S. Ikeda, "Acceleration of the EM algorithm," *Systems and Computers in Japan*, vol. 31, no. 2, pp. 10–18, February 2000.

[21] G. J. McLachlan and T. Krishnan, *The EM Algorithm and Extensions*, 2nd ed., ser. Wiley series in probability and statistics. John Wiley & Sons, Inc., 2008.